

Passive air exchanges between building and urban canyon via openings in a single façade

K. Syrios ^{*}, G.R. Hunt

Department of Civil and Environmental Engineering, Imperial College London, London SW7 2AZ, UK

Received 8 November 2006; received in revised form 3 May 2007; accepted 24 May 2007

Available online 10 July 2007

Abstract

The results of an experimental study examining the steady exchange of air and heat between a building and an urban canyon are presented. The focus is on the effect of the canyon aspect ratio on the airflow through openings made exclusively in one side of the building. The interaction of the external wind flow and the internal thermally-driven flow was shown to depend upon the ratio of the building height H_b to the canyon width W (distance between buildings forming the canyons). The trends observed as this aspect ratio (H_b/W) was varied allow for identification of canyon geometries that yield reduced or enhanced building ventilation airflow rates.

© 2007 Elsevier Inc. All rights reserved.

Keywords: Single-sided passive ventilation; Urban canyon; Laboratory modelling

1. Introduction

An urban canyon refers to the space formed by two typically parallel rows of buildings separated by a street and it forms the basic unit of modern cities. Passive, or natural, ventilation refers to the exchange of air between the interior of a building and the external environment that is driven by naturally-occurring pressure differences, i.e. without mechanical intervention. Convection induced by heat gains inside and incident on a building, and the action of wind provide the motive forces of natural ventilation, Etheridge and Sandberg (1996).

Airflows in urban canyons have been studied extensively as they provide a mechanism for pollutant dispersion, see, for example, the review by Vardoulakis et al. (2003). Besides the quality of outdoor air, indoor air quality (IAQ) has also received considerable attention in response to the increasing amount of time spent indoors by recent

generations and to a heightened awareness of links between health, productivity and IAQ. The movement of air and heat, or other pollutants, within a ventilated space plays a key role in determining the IAQ. Predicting this movement in naturally-ventilated buildings using laboratory and theoretical modelling techniques has formed the focus of a number of studies, see the review by Linden (1999), Hunt and Kaye (2006).

Urban settlements are exposed to urban flows. The surface pressure imposed by the external flow on building walls and roofs yields an additional driving force to supplement the thermally-driven natural ventilation. The driving wind-induced pressure difference depends on the opening locations, and on the surrounding urban geometry, Hussain and Lee (1980). The difference in surface pressure typically present between windward and leeward or side façades (Baturin, 1972; Orme et al., 1994) generally results in a robust pressure drop that tends to drive a cross-ventilation flow (Aynsley et al., 1977) within the enclosure when openings are made in more than one façade.

Designs of naturally-ventilated buildings often incorporate low-level and high-level openings in order to harness the stack effect (Etheridge and Sandberg, 1996) associated

^{*} Corresponding author. Tel.: +44 (0) 2075945990; fax: +44 (0) 2075945991.

E-mail addresses: constantine.syrios@imperial.ac.uk (K. Syrios), gary.hunt@imperial.ac.uk (G.R. Hunt).

with temperature differences between the interior and exterior environments. The typically warmer internal air rises to be exhausted through high-level openings. This outflow is balanced by an inflow of cooler ambient air through low-level openings. A so-called displacement flow is thereby established, Etheridge and Sandberg (1996).

Cross-ventilation of enclosures via a combination of high-level and low-level openings located in opposite (windward/leeward) façades in an urban canyon context has been studied experimentally by Syrios and Hunt (2007). We found that the presence of adjacent canyons can reverse the effect of the wind on the thermally-driven internal flow of an otherwise isolated building.

Occupied spaces situated in the urban environment often have access to the external environment via a single façade. The ventilation is then referred to as *single-sided* as air is expelled from the building and replacement air is drawn in to the building through a single side. Even for enclosures with openings on more than one façade, it may be preferential to limit connections to a single façade (e.g. linking to a courtyard), if, for example, the others link to polluted streets.

To date the internal (building) and external (canyon) flows have been studied mostly in isolation. The need to improve our understanding of their interaction and, in particular, of the exchanges between interior and exterior environments they induce provides the motivation for the current study. The effect of canyon flows on passive ventilation via high-level and low-level openings in a single side of a heated building is examined experimentally. Forced, rather than natural, single-sided ventilation has been studied experimentally and numerically by Moureh and Flick (2005). They found that, depending on the position of the horizontal inflow jet, a poorly ventilated region near the opposite wall may emerge.

The bulk of previous work on the natural ventilation of buildings has considered simplified building geometries and primarily isolated buildings as a means of enhancing understanding and predictive capability. As a starting point, flows within the simplified geometry of a single-spaced rectangular enclosure flanked by two symmetric urban canyons are studied herein. The ventilated building was empty. Detailed internal geometries (including furniture, appliances, etc.) have been considered in the comparative study of numerical models simulating thermally-driven ventilation alone by Jouvvray et al. (2007).

Each canyon aspect ratio H_b/W (building height to street width) examined resulted in the building being subject to a mean wind-induced pressure difference but with that mean pressure difference varying with canyon aspect ratio. Despite pressure fluctuations induced by the impingement and separation of the external flow on the canyon's sharp edges (see Syrios, 2005) a quasi-steady state was established for all H_b/W considered. This was verified by consecutive measurements. For a building subject to a mean wind-induced pressure difference the effects of varying the heat source strength, the wind speed and the open-

ing area (or building porosity) have been studied previously by Hunt and Linden (2001, 2005), Li and Delsante (2001), Gladstone and Woods (2001). The novelty of the current study lies in addressing the effect of changes in the external canyon geometry H_b/W on the ventilation flow and the known effects of heat source strength, wind speed and opening area are not reproduced herein.

In Section 2 the experimental technique applied to study the exchange of air and heat between building and canyon is outlined. Our experimental results that establish the effect of canyon airflows on single-sided building ventilation are given in Section 3 and the conclusions are drawn in Section 4. Arrows in figures indicate mean flow direction.

2. Methodology

The effect of neighbouring urban canyons on the single-sided ventilation of a building was studied using the 'salt-bath' technique: water was the working fluid and brine was used to achieve density differences. This technique has been used to successfully simulate thermally-driven building ventilation flows at small scale (Linden et al., 1990; Baker and Linden, 1991) and was extended by Hunt and Linden (1997, 2001) to include ventilation flows driven by combined thermal and wind forces.

By using brine, high Rayleigh number turbulent convection can be achieved at small scale. The reduced diffusivity of salt in water compared to the diffusivity of heat in air also ensures sufficiently high Peclet numbers despite the reduced model scale. Furthermore, the relatively large density differences that can be achieved by dissolving salt in water allow for high velocities through openings in the model and, hence, high Reynolds numbers. Approximate dynamical similarity can, thus, be achieved (Hunt and Linden, 1997) and measurements made in the laboratory provide useful insights to the flow at full scale and may be scaled to make predictions of, for example, airflow rates and thermal stratification.

A highly-insulated ventilated enclosure was represented by a clear Perspex box of length 598 mm and of 170 mm \times 170 mm vertical cross section (internal height $H = 150$ mm). Two plastic boxes of the aforementioned external dimensions were positioned with their long sides parallel to, and on either side of, the long side of the Perspex box. The three boxes were suspended in the test section of an 8.6 m long, 0.6 m wide and 0.6 m deep recirculating water-filled flume with their long sides spanning the flume width. In this way, two symmetric and inverted urban canyons were formed, see Fig. 1. The plastic boxes could be translated and locked at ten predetermined positions along horizontal plastic boards which formed the streets between the buildings so that the canyon aspect ratio H_b/W ('building' height to 'street' width) could be varied between 1/5 and 2. The ventilation of an isolated enclosure was studied simply by removing the two plastic boxes, in which case $H_b/W = 0$.

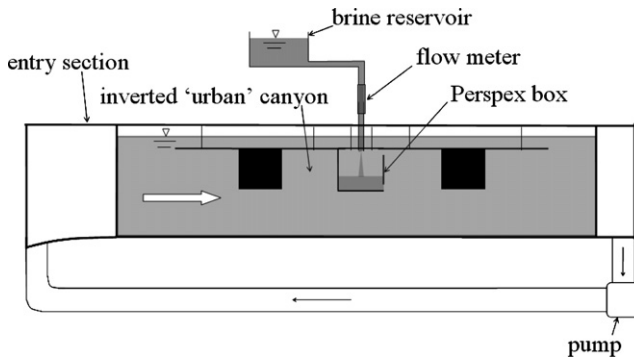


Fig. 1. Schematic of the experimental apparatus showing two (inverted) canyons formed by horizontal plastic boards and boxes (shaded in black) positioned on either side of the clear Perspex box.

A pump drove a recirculating flow in the flume, thereby, simulating wind in a direction perpendicular to the canyon streets. No attempt was made to simulate the atmospheric boundary layer.

A number of square-edged rectangular ventilation openings of height 1.5 cm, of either 2 or 4 cm width were positioned flush with the floor (low-level) and ceiling (high-level) in the vertical long sides of the Perspex box (of wall thickness 0.5 cm).

Internal heat gains were simulated by injecting saline solution from a brine reservoir (Fig. 1) at a constant rate into the Perspex box via a nozzle of diameter 5 mm. The continuous supply of solution, of constant salinity, generated a descending turbulent saline plume of constant buoyancy flux B ($\text{cm}^4 \text{s}^{-3}$). The saline plume is the analogue of a thermal plume in a building and the vertical inversion of the flow and model (Fig. 1) does not affect the flow dynamics for the small density differences considered (Baker and Linden, 1991). Dye was added to the supply to aid visualisation.

The saline stratification established by the plume in the Perspex box was visualised using a contact shadowgraph. Fluid densities within the Perspex box and flume were measured with a density meter (Anton Paar DMA 35N, accuracy $\pm 5 \times 10^{-4} \text{ g cm}^{-3}$). The large volume of water contained in the flume ensured that changes in its density ρ_a were negligible over the course of an experiment.

The steady two-layered stratification of the displacement flow pattern (Section 3, Figs. 3, 5 and 6) typically established by the localised input of buoyancy allowed for a visual inspection of trends in the steady ventilation flow

rate Q as the canyon aspect ratio was varied. The depth of the saline layer was clearly visible on the shadowgraph. The height h of the interface separating saline and fresh water layers (Fig. 2a) was measured directly on the shadowgraph (accuracy $\pm 2\text{--}4 \text{ mm}$). From the measurements of h trends in Q were inferred; an ascent (descent) of the steady density interface in the building, rather than laboratory, frame of reference corresponding to an increase (decrease) in Q (Linden et al., 1990).

Conservation of buoyancy flux for the enclosure gives the steady ventilation flow rate as

$$Q = \frac{B}{g'}, \quad (1)$$

where $g' = g(\rho - \rho_a)/\rho_a$ is the reduced gravity (or buoyancy) of the saline layer. The density of the (homogeneous) saline layer and, hence, of the fluid discharged from the Perspex box is denoted by ρ . The quantity Qg' denotes the (convective) buoyancy flux removed from the enclosure via the ventilation flow, which, in the steady state, equals the buoyancy flux input B assuming no buoyancy transfers with the building material (as is the case in the experiments).

3. Results

The main objective was to discern the effect of surrounding canyons on thermally-driven building flows by observing and measuring the response of the steady ventilation of the clear Perspex box to changes in H_b/W . Hence, the recirculation volume flow rate in the flume was maintained at a constant value $Q_{\text{rec}} = 0.0725 \text{ m}^3 \text{s}^{-1}$, giving a mean approach 'wind' speed of $V_{\text{wind}} = 20.1 \text{ cm s}^{-1}$ and a Reynolds number $\text{Re} \approx 1.4 \times 10^5$ indicating turbulent flow. Additionally, the plume buoyancy flux was fixed at $B = 133 \text{ cm}^4 \text{s}^{-3}$ – brine of $g'_{\text{source}} = 70 \text{ cm s}^{-2}$ was supplied at a constant rate $Q_{\text{source}} = 1.9 \text{ cm}^3 \text{s}^{-1}$. The area of the ventilation openings was also kept constant with $A_{\text{in}} = 6 \text{ cm}^2$ and $A_{\text{out}} = 3 \text{ cm}^2$ as the low-level and high-level opening areas, respectively. Taking discharge coefficients $C_{\text{din}} = C_{\text{dout}} = 0.6$ (Ward-Smith, 1980) gave an effective opening area as defined by Hunt and Linden (2005) of $A^* = [(2C_{\text{din}}^2 A_{\text{in}}^2)^{-1} + (2C_{\text{dout}}^2 A_{\text{out}}^2)^{-1}]^{-1/2} = 2.28 \text{ cm}^2$. Two opening configurations were considered, namely, openings exclusively in the windward façade (Fig. 2a) and openings

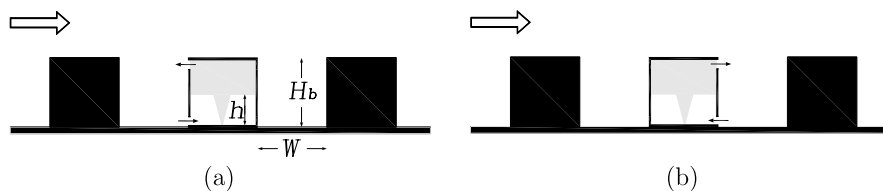


Fig. 2. Single-sided ventilation with normal approaching wind. (a) Openings in the windward façade and (b) openings in the leeward façade. The canyon or street width W , the building height H_b and the interface height h (set up by the plume for the displacement flows observed) are depicted.

exclusively in the leeward façade (Fig. 2b). The second configuration effectively corresponds to a reversal in the direction of wind for the first.

The frame of reference for the discussion hereafter is that of a building with a thermal plume rising from a heat source at floor level. Displacement flow was observed for

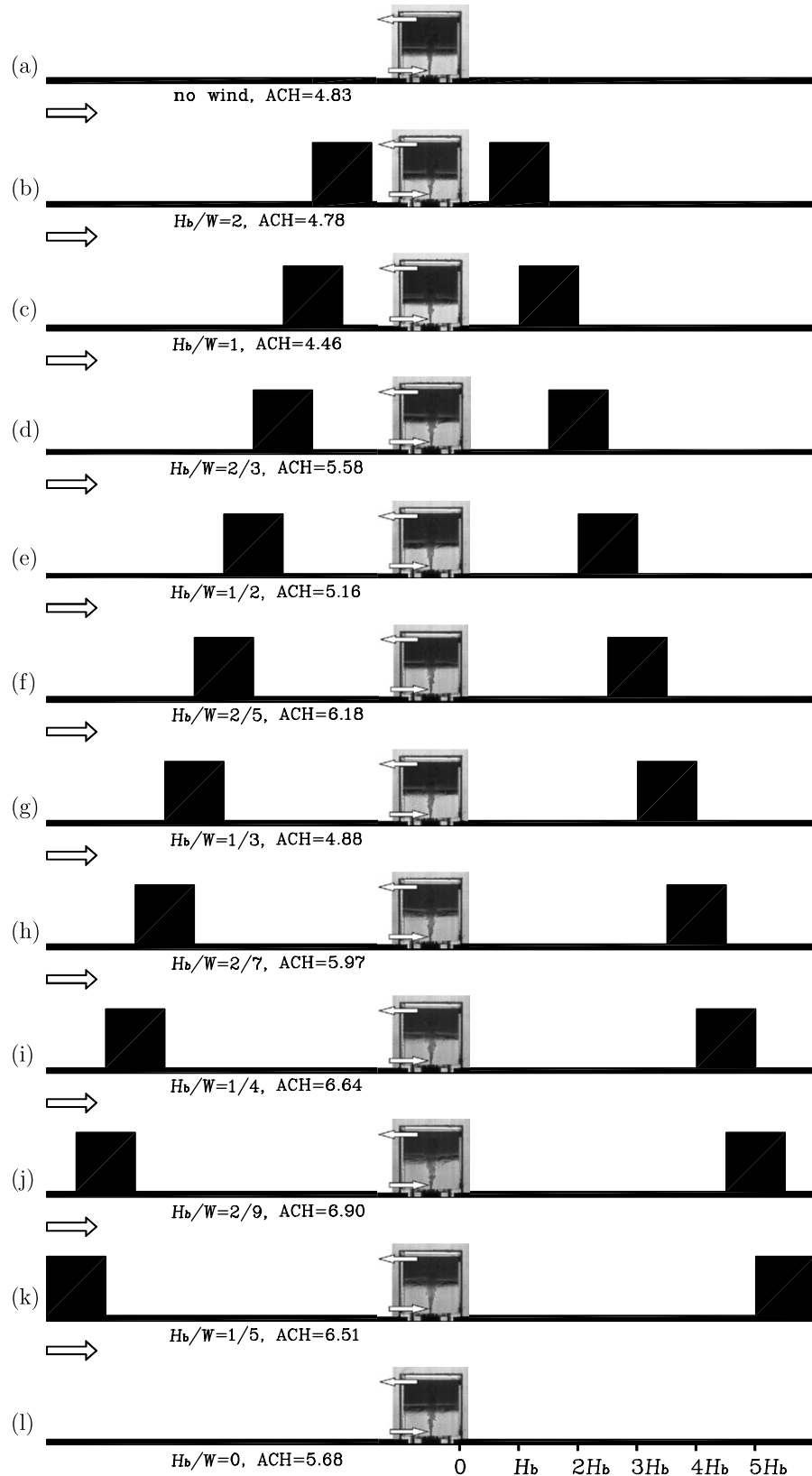


Fig. 3. Inverted shadowgraph images of the steady stratification for ventilation through windward openings for the entire range of H_b/W considered.

both opening configurations (Fig. 2), and maintained for the entire range of H_b/W examined. In each case inflow took place through the low-level vent, outflow through the high-level vent and a layer of approximately uniform buoyancy overlaid a layer at ambient density and of depth h .

Experimental results are presented in the form of non-dimensional interface height h/h_{nw} and non-dimensional upper-layer buoyancy g'/g'_{nw} , where the reference interface height $h_{nw} = 5.4$ cm and reference upper-layer buoyancy $g'_{nw} = 7.16$ cm s⁻² were measured in the absence of wind – the subscript ‘nw’ reads ‘no wind’. Error bars in the graphs of Figs. 4 and 7 indicate the experimental uncertainty associated with shadowgraph parallax errors (0.04–0.08 for h/h_{nw}) and instrument accuracy (0.07 for g'/g'_{nw}).

The steady ventilation flow rate Q was estimated for all H_b/W from (1) using the buoyancy measurements, see Appendix A. Volume flow rate estimates, expressed as the number of air changes per hour (ACH) for the ventilated box, are given in Figs. 3, 4c and 5 for windward openings, and Figs. 6 and 7c for leeward openings. ACH

is defined as the ratio of the total volume of air flushed from the enclosure in one hour to the volume of the enclosure.

The contribution of the source volume flux Q_{source} to Q was small: Q exceeded Q_{source} by a factor of at least 9 in all experiments, i.e. the bulk of the ventilation flow was due to plume entrainment and not to the volume flux input at the plume source.

3.1. Single-sided ventilation via windward openings

Fig. 3 depicts inverted shadowgraph images of the steady stratification that resulted when openings were located solely in the windward façade for the no-wind case and for wind flow past all eleven canyon aspect ratios considered. Purely buoyancy-driven flow (Fig. 3a) is independent of H_b/W as no external flow is involved. Despite the significant changes in the aspect ratio, the bulk features of the stratification and ventilation flow remained unchanged as is clearly evident in Fig. 3. However, as the

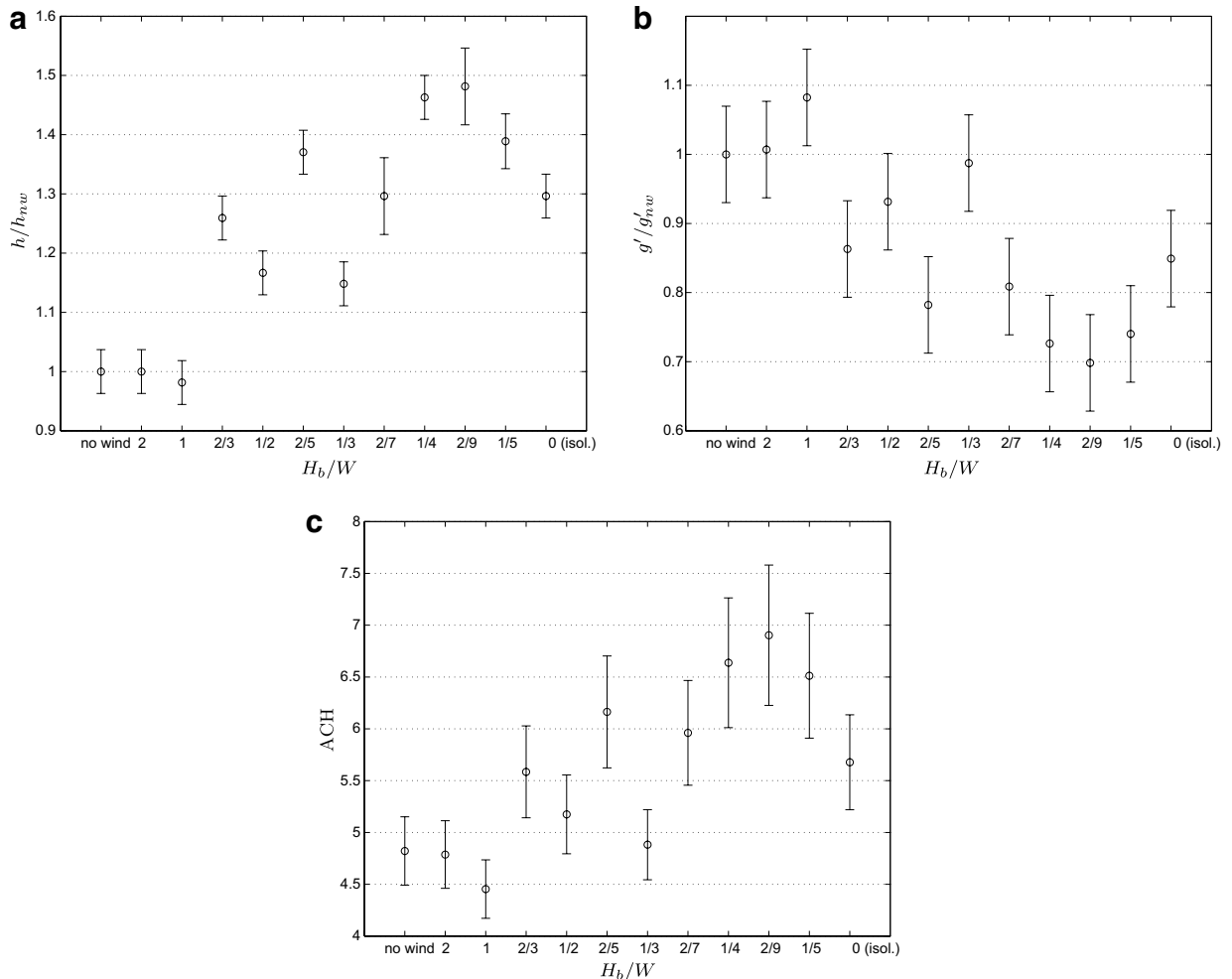


Fig. 4. Windward openings. For $H_b/W \leq 2/3$ an assisting effect of the canyon flow on the building’s ventilation is evident: (a) the steady interface ascended (h/h_{nw} vs. H_b/W), (b) the upper-layer buoyancy decreased (g'/g'_{nw} vs. H_b/W) and (c) ACH increased compared to purely buoyancy-driven flow (‘no wind’ data point) (ACH vs. H_b/W). For deeper canyons ($H_b/W \geq 1$) there is a subtle opposing effect of the wind.

volume flow rate in a plume increases with the distance from the source to the power of $5/3$, relatively small changes in the steady interface position yield relatively large changes in the ventilation flow rate and upper-layer buoyancy.

Interface height, upper-layer buoyancy and (inferred) ACH measurements are presented in Fig. 4. For $H_b/W \geq 1$ a subtle opposing effect of the wind (*cf.* Hunt and Linden, 2005) is evident from the slight interface height reduction (Fig. 4a) and increase in the upper-layer buoyancy (Fig. 4b) compared to purely buoyancy-driven flow ('no wind' data point). However, the magnitude of the interface and buoyancy departures from their no-wind values is small, the net effect of the canyon aspect ratio on wind pressure is weak and cannot be ascertained further.

For $H_b/W \leq 2/3$ the external flow tended to drive an upward flow through the space, *i.e.* in the same direction as and, thereby, assisting the buoyancy-driven flow. The resulting ascent of the interface (Fig. 4a) resulted in the plume supplying the upper layer with air of reduced buoyancy (cooler air) as a consequence of having entrained air at ambient temperature over an increased height. The buoyancy of the upper layer decreased (Fig. 4b) and ACH values increased accordingly (Fig. 4c). Based on these measurements, the maximum ventilation flow rate was recorded when the building was surrounded by shallow canyons – the ventilation flow rate for $H_b/W = 2/9$ exceeding that through an isolated enclosure by over 40%.

The shadowgraph images of Figs. 3c ($H_b/W = 1$) and 3j ($H_b/W = 2/9$) are shown magnified in Fig. 5 to highlight the difference in internal stratification resulting from different canyon geometries. For $H_b/W = 2/9$ the increased interface height is consistent with the increased ACH achieved (*cf.* Linden et al., 1990).

Although the approaching wind speed, the magnitude of the heat input and the opening area were kept constant (their specific values chosen for convenience and illustrative purposes), changing their values is not expected to alter the basic trends in the response of the steady ventilation flow

to changes in H_b/W for the turbulent flows anticipated. For example, the wind-induced pressure drop imposed externally across the openings will assist/oppose the buoyancy-driven flow, irrespective of the magnitude and spatial distribution of the internal heat gains.

The assisting wind effect deduced for relatively shallow canyons ($H_b/W \leq 2/3$) can be explained in terms of the 'S'-shaped surface pressure distribution on the windward wall pertaining to the wake interference flow and, in particular, the isolated roughness flow regime, see the wind-tunnel studies of Soliman (1976), Lee and Soliman (1977), Hussain and Lee (1980). The high-level opening is near the roof edge where the flow accelerates as it passes over the building, thereby, resulting in relatively low surface pressures. In contrast, there is a pressure build-up near the ground, where the low-level opening is located. For illustrative purposes, the expected external flow pattern and surface pressure distribution on the windward wall are sketched for $H_b/W = 1/5$ in Appendix B (Fig. B.1a).

For deeper canyons ($H_b/W > 2/3$), the skimming flow regime is expected to be present with the windward wall's pressure distribution resembling a reverse 'C' (Soliman, 1976; Lee and Soliman, 1977; Hussain and Lee, 1980) and with pressures near the upper (convex) edge higher than near the lower (concave) edge. This is in broad agreement with the (subtle) opposing canyon flow effect observed herein. In general, as H_b/W increases from zero, the stagnation point on the windward wall moves upwards and there is a shift in the surface pressure distribution from the 'S' shape of the isolated roughness flow to the reverse 'C' shape of the skimming flow, see Hussain and Lee (1980) and the cavity flow studies of Mills (1961), Tani et al. (1961), Kistler and Tan (1967). Due to the subsequent increase in pressure in the region of the upper vent, the canyon flow alone would tend to drive inflow through the vent, thus, opposing the thermally-driven flow.

3.2. Single-sided ventilation via leeward openings

The steady-state stratifications established when the openings were located in the leeward façade alone are shown in the inverted shadowgraph images of Fig. 6 for the entire range of H_b/W considered. The changes to the interface height and the upper-layer buoyancy upon introduction of the canyon flow were less dramatic than for openings located in the windward façade. Displacement flow was again maintained and a maximum flow rate was achieved when the building received a degree of sheltering by the canyons, this time for $H_b/W = 1$. For an isolated enclosure and identical wind speeds, a greater ventilation flow rate was achieved with openings in the windward façade than in the leeward façade (*cf.* Figs. 3(1) and 6(1)).

Measurements of the steady interface height and upper-layer buoyancy, and inferred values of ACH are presented

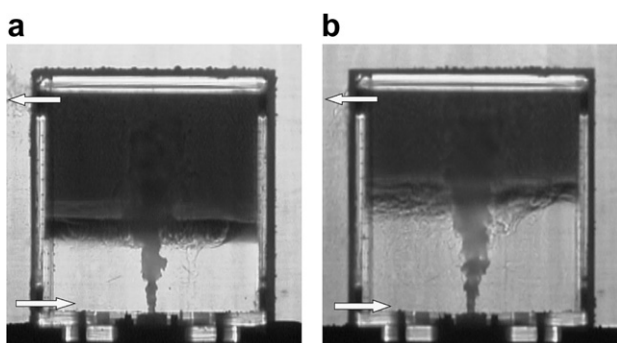


Fig. 5. Inverted shadowgraph images of the steady stratification established for ventilation through windward openings for (a) $H_b/W = 1$, $ACH = 4.46$ and (b) $H_b/W = 2/9$, $ACH = 6.90$. The increased interface height evident for $H_b/W = 2/9$ is accompanied by a reduction in upper-layer buoyancy (Fig. 4b) and an increase in ventilation flow rate.

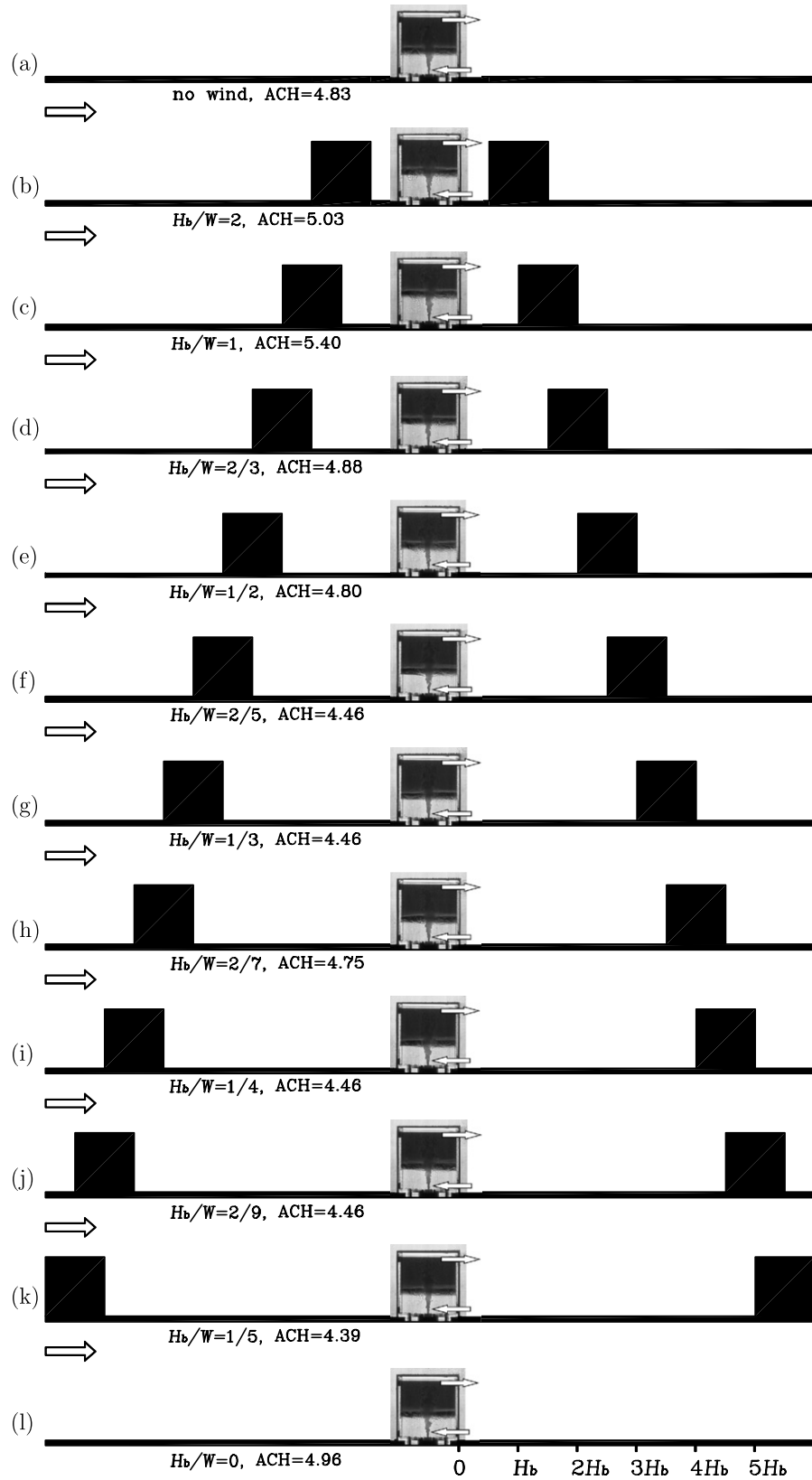


Fig. 6. Inverted shadowgraph images of the steady stratification for ventilation through leeward openings for the entire range of H_b/W considered.

in Fig. 7. An assisting effect of the canyon flow is evident for $H_b/W \geq 2/3$ by the raised interface (Fig. 7a) and the

reduced buoyancy (Fig. 7b) compared to the purely buoyancy-driven flow ('no wind' data point). For $H_b/W \leq 1/2$

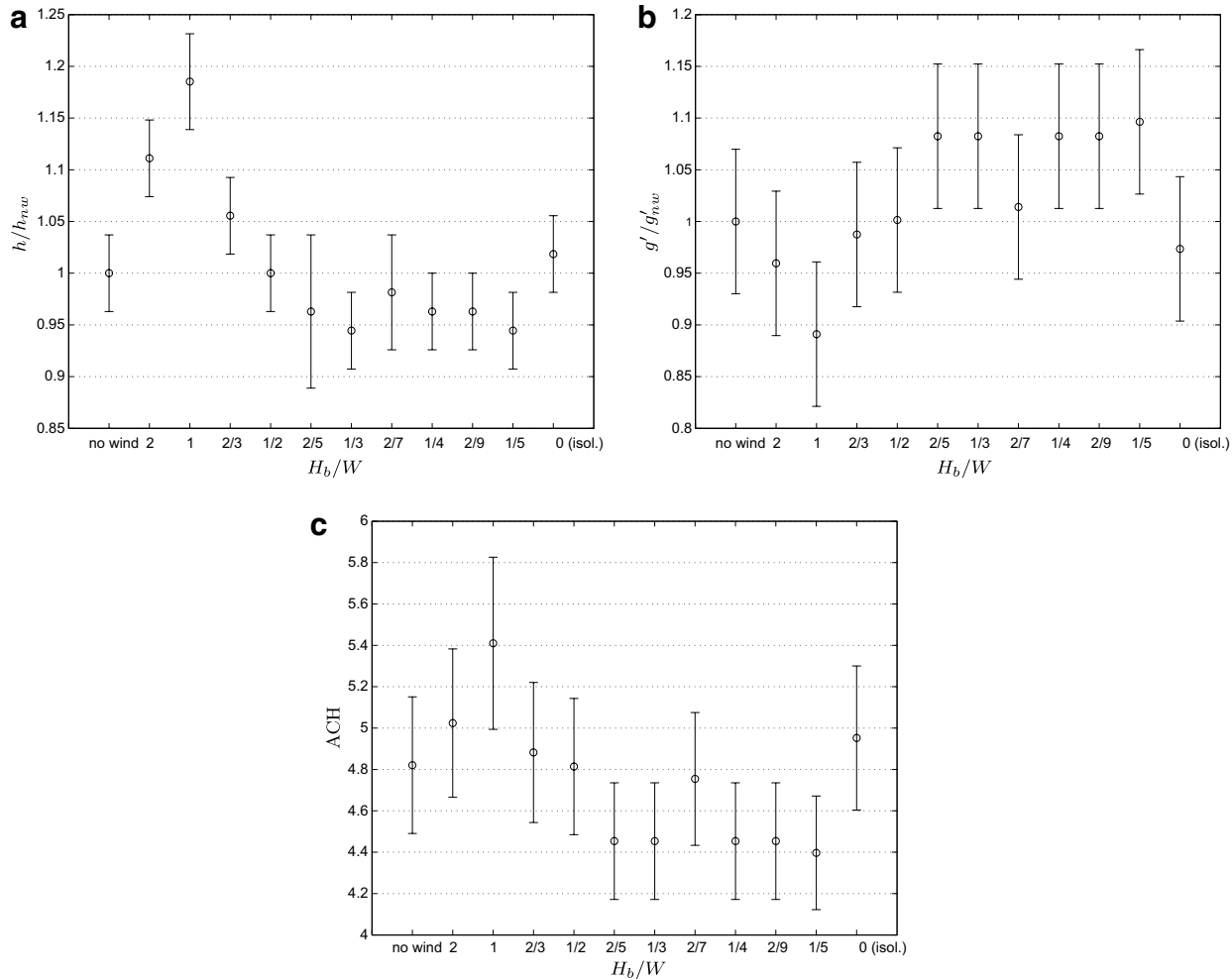


Fig. 7. Leeward openings. For $H_b/W \geq 2/3$ an assisting effect of the wind is evident: (a) the steady interface ascended (h/h_{nw} vs. H_b/W), (b) the upper-layer buoyancy reduced (g'/g'_{nw} vs. H_b/W) and (c) ACH increased compared to purely buoyancy-driven flow ('no wind' data point) (ACH vs. H_b/W). For shallower canyons ($H_b/W \leq 1/2$) there is no clear trend.

the effect of the external flow is subtle and there is no clear trend: for $H_b/W = 1/2$ there was virtually no deviation from purely buoyancy-driven flow, for $1/5 \leq H_b/W \leq 2/5$ a weak opposing effect was observed and for $H_b/W = 0$ a slight assisting effect was present. These variations are reflected in the ACH values (Fig. 7c).

The assisting wind effect for relatively deep canyons ($H_b/W \geq 2/3$) can be explained in terms of the surface pressure distribution on the leeward wall. For the skimming flow present at these aspect ratios, the external flow 'skims' the rooftops creating a zone of fluid acceleration close to the leeward wall at high level due to entrainment of fluid from the canyon. This results in relatively low pressure in this region. The low pressure is evident in the measurements of Soliman (1976) and in the cavity flow study by Mills (1961), while Freitas et al. (1985) report the presence of a recirculation bubble in the same region in their lid-driven cavity flow. The surface pressure at the low-velocity region close to ground level exceeds the pressure at high level, thus, tending to drive inflow through the

low-level vent and outflow through the high-level vent and, thereby, assisting the buoyancy-driven flow. For illustrative purposes, the expected external flow pattern and surface pressure distribution on the leeward wall are sketched for $H_b/W = 1$ in Appendix B (Fig. B.1b).

For shallower canyons ($H_b/W \leq 1/2$) the wake interference and isolated roughness flow regime are more likely to be present. The pressure distribution on the leeward wall is then close to uniform, Soliman (1976), Lee and Soliman (1977), Hussain and Lee (1980). This is in broad agreement with the subtle effect of the external flow on the buoyancy-driven flow that does not exhibit a clear trend.

4. Conclusions

The effect of urban canyon flows on the steady single-sided passive ventilation of a canyon building with internal heat gains was studied experimentally using small-scale

models in water, and brine to create density differences. The wind was directed perpendicularly to the canyon street. Ventilation via openings solely in the windward façade and via openings solely in the leeward façade was considered – in each case with ventilation openings at both high and low level in the façade. The canyon width was varied between one half of the building height and five times the building height. To the authors' knowledge, this is the first time this modelling approach has been applied to examine the influence of canyon geometry on single-sided passive building ventilation.

From the variation of the depth and buoyancy of the upper layer from their steady values established under no-wind conditions the following can be deduced: for canyons with aspect ratio $H_b/W > 2/3$ natural ventilation is enhanced¹ for openings in the leeward façade; for shallower canyons natural ventilation is enhanced for openings in the windward façade. These findings are consistent with independent surface pressure distributions presented in the literature.

The effect of the urban canyon on the single-sided passive ventilation of an otherwise isolated building was overall relatively small. Ventilation through the leeward façade provided less deviation from purely buoyancy-driven flow than ventilation through the windward façade. Displacement flows, as established by a localised heat source in the building under no-wind conditions, were maintained when wind blew past the canyon for all canyon aspect ratios considered. This was due to the relatively small wind-induced pressure drops achieved between openings located in a single building façade compared with pressure drops achieved across openings in, for example, windward and leeward façades. The (small) magnitude of the wind-induced pressure drop was attributed to the opening arrangement and not to the value of the approaching wind speed. An identical wind speed relative to the buoyancy-induced velocity generated sufficiently high pressure drops during the cross-ventilation experiments of [Syrios and Hunt \(2007\)](#) to break down the stratification established by displacement flow and incite flow reversal (i.e. a mixing flow for identical buoyancy flux and opening area).

Acknowledgements

The authors gratefully acknowledge the financial support of the BP Advanced Energy Programme in Buildings at Imperial College London. KS is grateful to the Alexander S. Onassis Public Benefit Foundation and the Eugenides Foundation. We would like to thank Professor J.M.R. Graham of the Department of Aeronautics, Impe-

Table A.1

Steady ventilation flow rates Q through the ventilated box tabulated against the canyon aspect ratio H_b/W for windward and leeward opening configurations as shown in [Fig. 2](#)

H_b/W	Q ($\text{cm}^3 \text{s}^{-1}$)	
	Windward openings	Leeward openings
No wind	18.6	18.6
2	18.4	19.4
1	17.2	20.8
2/3	21.5	18.8
1/2	19.9	18.5
2/5	23.8	17.2
1/3	18.8	17.2
2/7	23.0	18.3
1/4	25.6	17.2
2/9	26.6	17.2
1/5	25.1	16.9
0	21.9	19.1

rial College London for providing access to their Hydrodynamics Laboratory.

Appendix A. Ventilation flow rate estimates

The steady ventilation flow rate Q ($\text{cm}^3 \text{s}^{-1}$) through the Perspex box was estimated from conservation of buoyancy flux (1) using the buoyancy measurements. [Table A.1](#) summarises these estimates. The Q values are expressed in air changes per hour (ACH) in [Figs. 3, 4c, 5, 6 and 7c](#), where

$$\text{ACH} = 3600Q/V \quad (\text{A.1})$$

and $V = 13872 \text{ cm}^3$ denotes the internal volume of the Perspex box.

Appendix B. External flow sketches

For shallow canyons ($H_b/W \leq 2/3$) the wind had an assisting effect on the passive ventilation when openings were in the windward façade. When openings were made in the leeward façade an assisting effect was achieved only with deeper canyons. Schematics of the expected external flow patterns are shown in [Fig. B.1](#) for the two aspect ratios $H_b/W = 1/5$ (shallow canyon) and 1 (deep canyon). According to [Oke \(1988\)](#), for $H_b/W = 1/5$ an isolated roughness flow regime is expected and for $H_b/W = 1$ a skimming flow is expected.

Based on the measurements of [Hussain and Lee \(1980\)](#), the anticipated surface pressure distribution on the façades that yield enhanced ventilation flow when they bear the openings – windward façade for the shallow canyon and leeward façade for the deep canyon – is drawn qualitatively (pressure coefficient C_p curves). For the shallow canyon see [Fig. B.1a](#) and for the deep canyon see [Fig. B.1b](#). Both distributions yield greater surface pressure near the ground than near the roof, which supports the assisting wind effect discussed in [Section 3](#).

¹ Enhanced ventilation refers to increased airflow rates and reduced temperatures within the building.

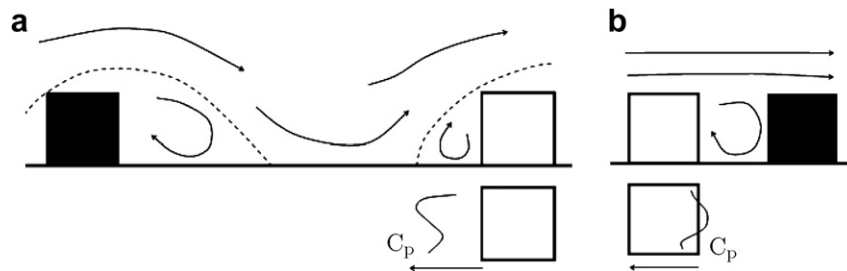


Fig. B.1. For the two indicative aspect ratios selected, (a) $H_b/W = 1/5$ and (b) $H_b/W = 1$, schematics of expected airflow pattern following Oke (1988) and surface pressure distribution (pressure coefficient C_p curves) following Hussain and Lee (1980) are presented. In (a) the dotted lines indicate the extent of regions of flow separation.

References

Aynsley, R.M., Melbourne, W., Vickery, B.J., 1977. *Architectural Aerodynamics*. Applied Science Publishers Ltd., London.

Baker, N., Linden, P.F., 1991. *Atrium Buildings Architecture and Engineering*. CICC Publications, Welwyn, England, Ch. Physical Modelling of Airflows – A New Design Tool, pp. 13–22.

Baturin, V.V., 1972. Fundamentals of industrial ventilation. In: International Series of Monographs in Heating, Ventilation and Refrigeration, third ed. Pergamon Press Ltd., Oxford.

Etheridge, D.W., Sandberg, M., 1996. *Building Ventilation: Theory and Measurement*. John Wiley & Sons, Chichester.

Freitas, C.J., Findikakis, A.N., Street, R.L., 1985. The physics of three-dimensional cavity flow. In: Taylor, C. (Ed.), *Proceedings of the 4th International Conference on Numerical Methods on Laminar and Turbulent Flow*, Swansea, UK, pp. 503–514.

Gladstone, C., Woods, A.W., 2001. On buoyancy-driven natural ventilation of a room with a heated floor. *J. Fluid Mech.* 441, 293–314.

Hunt, G.R., Kaye, N.B., 2006. Pollutant flushing with natural displacement ventilation. *Build. Environ.* 41, 1190–1197.

Hunt, G.R., Linden, P.F., October 1997. Laboratory modelling of natural ventilation flows driven by the combined forces of buoyancy and wind. In: *Proceedings of the CIBSE National Conference London*, UK, pp. 101–107.

Hunt, G.R., Linden, P.F., 2001. Steady-state flows in an enclosure ventilated by buoyancy forces assisted by wind. *J. Fluid Mech.* 426, 355–386.

Hunt, G.R., Linden, P.F., 2005. Displacement and mixing ventilation driven by opposing wind and buoyancy. *J. Fluid Mech.* 527, 27–55.

Hussain, M., Lee, B.E., 1980. An investigation of wind forces on three dimensional roughness elements in a simulated atmospheric boundary layer flow. Part II: flow over large arrays of identical roughness elements and the effect of frontal and side aspect ratio variations. *Tech. Rep. BS 56*, Department of Building Science, Faculty of Architectural Studies, University of Sheffield.

Jouvron, A., Tucker, P.G., Liu, Y., 2007. On nonlinear RANS models when predicting more complex geometry room air flows. *Int. J. Heat Fluid Fl.* 28, 275–288.

Kistler, A.L., Tan, F.C., 1967. Some properties of turbulent separated flows. *Phys. Fluid. Suppl.* 10, S165–S173.

Lee, B.E., Soliman, B.F., 1977. An investigation of the forces on three dimensional bluff bodies in rough wall turbulent boundary layers. *J. Fluid. Eng.-T. ASME* 99, 203–510.

Li, Y., Delsante, A., 2001. Natural ventilation induced by combined wind and thermal forces. *Build. Environ.* 36, 59–71.

Linden, P.F., 1999. The fluid mechanics of natural ventilation. *Annu. Rev. Fluid Mech.* 31, 201–238.

Linden, P.F., Lane-Serff, G.F., Smeed, D.A., 1990. Emptying filling boxes: the fluid mechanics of natural ventilation. *J. Fluid Mech.* 212, 309–335.

Mills, R.D., 1961. *Flow in Rectangular Cavities*. Ph.D. Thesis, University of London, UK.

Moureh, J., Flick, D., 2005. Airflow characteristics within a slot-ventilated enclosure. *Int. J. Heat Fluid Fl.* 26, 12–24.

Oke, T.R., 1988. Street design and urban canopy layer climate. *Energ. Buildings* 11, 103–113.

Orme, M., Liddament, M., Wilson, A., March 1994. An analysis and data summary of the AIVCs numerical database. Technical Note AIVC 44, Air Infiltration and Ventilation Centre, University of Warwick, Coventry, UK.

Soliman, B.F., 1976. *A Study of the Wind Pressure Forces acting on Groups of Buildings*. Ph.D. Thesis, Department of Building Science, University of Sheffield, UK.

Syrios, K., 2005. *Natural Ventilation of Buildings in Urban Canyons*. Ph.D. Thesis, University of London, UK.

Syrios, K., Hunt, G.R., 2007. Urban canyon influence on building natural ventilation. *Int. J. Ventilation* 6, 43–50.

Tani, I., Iuchi, M., Komoda, H., 1961. Experimental investigation of flow associated with a step or a groove. Technical Report 364, Aeronautical Research Institute, University of Tokyo.

Vardoulakis, S., Fisher, B.E.A., Pericleous, K., Gonzalez-Flesca, N., 2003. Modelling air quality in street canyons: a review. *Atmos. Environ.* 37, 155–182.

Ward-Smith, A.J., 1980. *Internal Fluid Flow: The Fluid Dynamics of Flow in Pipes and Ducts*. Clarendon Press, Oxford.